

Overview of the flare index during the maximum phase of the solar cycle 23

T. Ataç^{a,*}, A. Özgüç^a, J. Rybák^b

^a *Kandilli Observatory and E.R.I., Boğaziçi University, Çengelköy, 34684, Istanbul, Turkey*

^b *Astronomical Institute of the Slovak Academy of Sciences, 05960 Tatranská Lomnica, Slovak Republic*

Received 8 October 2004; received in revised form 17 January 2005; accepted 17 January 2005

Abstract

A brief description and final results of the flare index of solar activity for the maximum phase of the cycle 23 are given. The patterns of similar activity indices that arise under different physical conditions during the cycle 23 were compared with the flare index. The intermediate-term periodicities in the daily flare index data for the full disc and for the northern and the southern hemispheres of the Sun were calculated before by the authors using the Fourier transform, and it was found that 64, 125 days periodicities are in operation during the maximum phase of the solar cycle 23. In this paper, we examined these periodicities in time domain by using the wavelet transform. The results of this transform show that during the maximum phase of the current solar cycle a very prominent multi-peaked structures exist in each solar hemisphere and the occurrence of flare index power is highly intermittent in time. Moreover, it is found that the flare activity of the opposite hemispheres were not well time-synchronized during the maximum phase. The flare activity of the southern hemisphere was observed to be more dominant in determining the characteristics of the flare activity in the solar cycle 23.

© 2005 COSPAR. Published by Elsevier Ltd. All rights reserved.

PACS: 96.60.Rd; 96.60.Ly

Keywords: Solar activity; Flares; Wavelet analysis; Periodicity

1. Introduction

Solar activity covers a range of phenomena at all levels in the solar atmosphere and time-scales ranging from seconds and minutes, through months, to the 11- or 22-year solar activity cycle. According to new observations immense cracks sometimes develop in Earth's magnetosphere and remain open for hours during the bad space weather conditions. This usually happens in the course of solar cycle maximum. Highly variable conditions in the geospace environment and those on the Sun persist throughout the maximum phase of solar activity.

Expressing aspects of that activity in terms of single indices is useful in investigating its role as a driver for various space and terrestrial phenomena.

Solar physicists have tried to quantify the variation of solar activity with time, beginning with Wolf's classical formula for the relative numbers of sunspots. An index of solar activity is a quantity intended to describe some aspect of activity for the Sun as a whole. Being able to express aspects of that activity by many indices, such as the Wolf number, the 2800 MHz radio flux, X-ray and EUV indices, cosmic-ray flux, etc., is useful for studying the Sun's long-term behaviour and its interaction with our near Earth space environment. The longest continuous record of solar activity is the regular sunspot observations. As well as in many studies in the solar-terrestrial field, solar flares are classified as one of the

* Corresponding author. Tel.: +90 21 6308 0514.

E-mail addresses: atac@boun.edu.tr (T. Ataç), ozguc@boun.edu.tr (A. Özgüç), choc@astro.sk (J. Rybák).

most important solar events affecting the Earth. Kleczek (1952) introduced the quantity $Q = i t$ to quantify the daily flare activity over a 24-h period. He assumed that this relationship roughly gave the total energy emitted by the flare and named it “flare index” (FI). In this relation, “ i ” represents the intensity scale of importance of a flare in $H\alpha$ and “ t ” the duration in $H\alpha$ (in minutes) of the flare. The determination of Q has been explained previously (Özgüç et al., 2003). Calculated values are available for general use in anonymous ftp servers of our observatory¹ and NGDC².

In this paper, the results of the determination of the flare index for the solar cycle 23 are presented. The amplitude of the 23rd solar cycle for similar activity indices with the amplitude of the previous cycle was compared in Section 2. Midrange periodicities in solar flare occurrence during the maximum phase of the cycle 23 are examined using wavelet transform (WT) in Section 3 and discussion and concluding remarks are presented in Section 4.

2. The amplitude of the solar cycle 23

We compared the amplitudes of the cycles 22 and 23 by using similar activity indices which are produced at different layers in the solar atmosphere and by different processes. Each of them reflects different physical conditions in the solar atmosphere. The indices to be selected are as follows:

1. The mean solar magnetic field (MMF). Stanford University, Wilcox Solar Observatory measures the net magnetic field intensity in microteslas summed over the disk. Such integrated light measurements have been made daily since May 1975 (Scherrer et al., 1977) (<http://quake.stanford.edu/wso/wso.html>).
2. Daily corrected total areas of sunspot groups (TSA). These are observed, measured and compiled by USAF/NOAA (<http://science.msfc.nasa.gov/ssl/pad/solar/greenwch.htm>).
3. The relative sunspot number (RSN). This is an index of the activity of the entire visible disk of the Sun calculated by the Sunspot Index Data Center (<http://sidc.oma.be/index.php3>).
4. A composite record of the Sun’s total irradiance (IR) is compiled from measurements made by five independent space-based radiometers since 1978. We used the Version 26 of that data set. More information about the determination of this composite can be found in the paper of Fröhlich and Lean (1998) (<ftp://ftp.pmodwrc.ch/data/irradiance/composite/>).

5. Coronal index (CI) introduced by Rybansky (1975) represents the total irradiance of the green corona emitted from the Sun’s visible hemisphere (<http://www.ngdc.noaa.gov/stp>).

In all the activity indices the amplitude of the current cycle in the same time interval is distinctively weaker than the previous one except of the total solar irradiance as it can be seen from Fig. 1. The cycle 23 violates the well known rule that the odd cycles are more active than the preceding even ones. Recently, Komitov and Boney (2001) showed that violation of the Gnevyshev-Ohl rule could not be random phenomena but occurring under special conditions, the main factor being the very high maximum of the even-numbered cycle. Hence, they conclude that the strong G-O rule violation in the cycle 23 suggests the onset of a solar activity minimum caused by the declining phases of both the 100 and 200 years solar cycles. In fact, the weaker present 11-year cycle is not completely unexpected. The methods for predicting the cycle’s amplitude are widely reviewed in a recent paper by Schatten (2003). One of these new prediction techniques was the one proposed by Ahluwalia (1998) which is based on the annual mean value of Ap observed 1 year into the new cycle onset. It seems to work for the last six cycles (17–22). This technique also predicted successfully that the cycle 23 would be lower than the cycles 17 and 20.

Another proposal to explain the weakness of the solar cycle 23 was given by Schatten (2003). He draws our attention to the new interpretation of the Babcock solar dynamo. In this model, the Sun’s polar fields near solar minimum are wrapped up by the differential rotation to form the toroidal fields, which later float to the Sun’s surface and erupt to form active regions where flares are formed. Hence, over an 11-year solar cycle, the amplification sometimes regenerates more polar field and sometimes less. By monitoring the observed magnetic fields on the Sun one can use these observations for predicting amplitudes of the future solar cycles. Based on this, they have created a new solar index called the Solar Dynamo Amplitude (SODA index) which represents the strength of the Sun’s buried magnetic flux. In his paper Schatten showed that the time variations of the SODA index has been gradually decreasing in the cycle 22 which would later explain the decrease in the amplitude in the cycle 23.

3. Periodicities in solar flare index during the maximum phase

First results on these periodicities will be published elsewhere. The most pronounced power peaks found by Fourier transform (FT) are 64 and 125.9 days for the full disc and for the northern hemisphere, and 83

¹ ftp://ftp.koeri.boun.edu.tr/pub/astronomy/flare_index.

² ftp://ftp.ngdc.noaa.gov/STP/SOLAR_DATA/SOLAR_FLARES/INDEX.

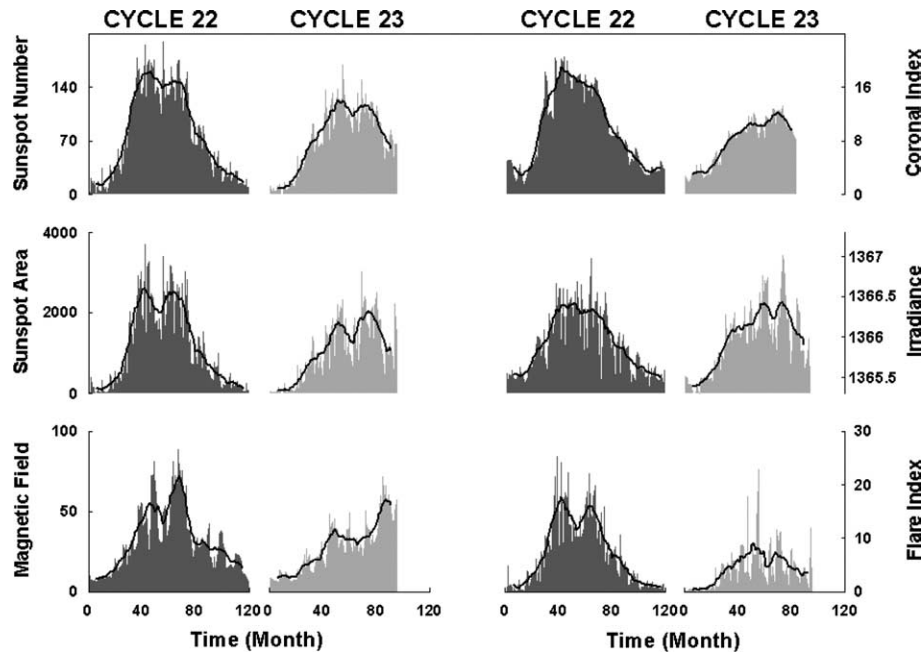


Fig. 1. Comparison of the similar activity indices for the previous and the current cycles. Dark areas show monthly means and solid lines show 11-month running means of those indices.

and 125.9 days for the southern hemisphere of the Sun. Since the peak around 80 days was not very prominent in the results of WT power spectrum, therefore, we omit this periodicity hereafter. Classical Fourier transform analysis allows a study of a signal only in the frequency domain whereas WT analysis yields information in both time and frequency domains (e.g., Daubechies, 1990; Kumar and Faufoula-Georgiou, 1997). Therefore, we have also applied wavelet analysis to a time series consisting of daily flare index between 1 January 1999 and 31 December 2002 to study the temporal variation with time scales of intermediate-term periods. These three time series (full disc's, northern and southern hemispheres) were smoothed with 7-day running means before the WT calculations. The algorithm of the continuous wavelet transform was applied after Torrence and Compo (1998) within the period range 40–200 days. The Morlet wavelet, a plane sine wave with an amplitude windowed in time by a Gaussian function, has been selected to search for variability at different frequencies over the whole length of the time series. The non-dimensional frequency has been set to 6 which fixed the length of all wavelets according to their scales. The calculated wavelet power spectrum is suppressed on the edges of the time domain within the cones of incidence due to the applied WT algorithm. The significance levels of the calculated WT power were derived using the null hypothesis according to Torrence and Compo (1998) assuming that noise was distributed independently on periods. The 99% confidence level, used in this study, implies that 5% of the wavelet power should be

above this level for each period. Figs. 2–4 show the time-period diagram of the WT power spectrum (power in arbitrary units) of the northern and southern hemispheres and the full disc flare index for the whole epoch studied.

Fig. 2 shows behaviour of the WT power for the northern hemisphere in which all peaks are centred around the FI power burst at 2000.3–2000.5. Merging these two peaks of FI with other FI enhancements before and after them produced a lot of power almost in the whole period range under study. There is no power enhancement for the periods around 64 days which was detected by FT except three weaker pulses at 1999.8, 2000.6, and 2001.9. For the southern hemisphere the WT results shown in Fig. 3 display the power around 120 days which reaches a peak value located at 1999.8. This comes from repetition of the flare index enhancements at 1999.5–1999.9 and at 2000.1–2000.4. The power peak around 60 days located at 2000.5 comes from the repetition of the FI peak located at 2000.6 and the two side maxima located at 2000.4 and 2000.7. The peak around 80 days was not very prominent in WT power at 2001.6 and additionally this period was identified also at 1999.8 at the same time as the peak at 120 days. Finally, results of the WT for the whole disc can be seen in Fig. 4. A mess of different waves of the two hemispheres with different phases have produced the several other peaks in the WT power spectrum. The broad peak around 120-day which is related to the FI peaks located between 1999.4–1999.7 and between 2000.1–2000.4, is rich in periods. The most significant

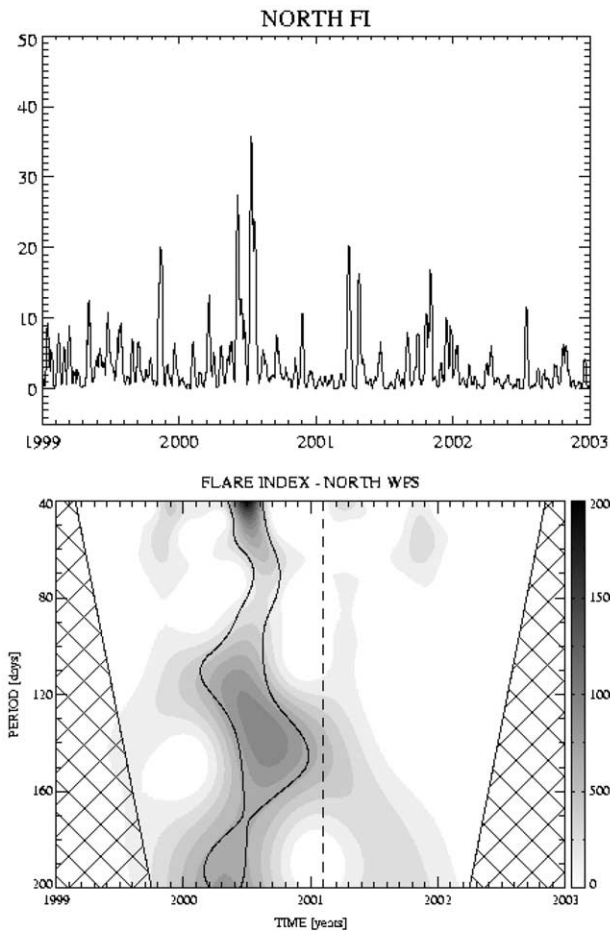


Fig. 2. The 7-day running mean of the flare index (upper panel), and the wavelet power spectrum of the daily flare index of the northern hemisphere of the Sun for the period range 40–200 days. Grey-scale coding of power from white to black represents the square root of power in a linear scale given on the right side bar. The solid curve shows the 95% confidence levels of the local power above the noise level assuming noise independence on periods. The cone of incidence is marked by the crosshatched regions.

peak comes from the nearly rotation repetition of the FI around the year 2000.5 in three consecutive rotations.

Wavelet analysis results showed that the flare activity of the opposite hemispheres were not well time-synchronized during the maximum phase. The flare activity of the southern hemisphere was observed to be more dominant in determining the characteristics of the flare activity in the solar cycle 23.

4. Discussion and conclusion

We have studied temporal variations of the flare index considering the FI for the maximum phase of the solar cycle 23. We examined, in the FI data, the reality of solar periodicities concentrating on periods between 40 and 200 days. During this time periods FI shows some

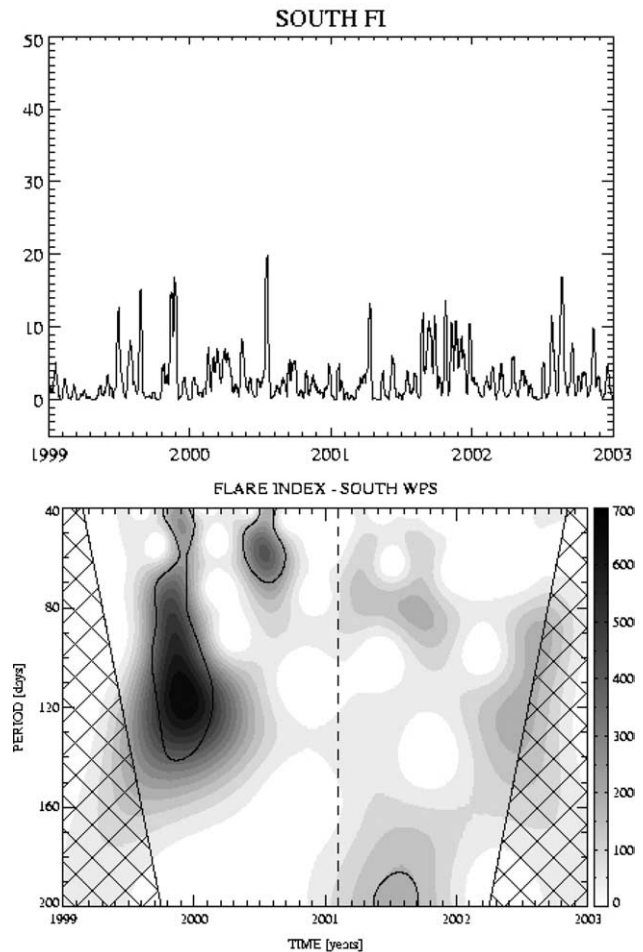


Fig. 3. The 7-day running mean of the flare index (upper panel) and the wavelet power spectrum of the daily flare index of the southern hemisphere of the Sun. Details are as Fig. 2.

periodicities which are 64 and 125 days. The 64-day periodicity has been detected only during the current cycle. Caballero and Valdes-Galicia (2001) found this periodicity in sunspot number, hard X-ray flux and cosmic ray intensity for the time interval of 1990–1999.

Lou et al. (2003) reported mid-term quasi periodicities in X-ray flares of class $\geq M5.0$ using four-year data 1999–2003. Their Fourier power spectral analysis gave significant periods at 157, 122, 98 and 34 days in X-ray solar flares. Recently, midrange periodicities in solar flare occurrence (X-ray flares of class $\geq M1.0$) have been analyzed by Bai (2003). He found that 129 and 33.5 days periodicities were in operation for the interval from 9 September 1999 to 5 June 2001, during which the five epochs of high activity were identified. The appearance of the period nearly 120 days in our analysis reminded us the idea that 25.5 days is a fundamental period of the Sun, and solar flare activity often exhibits periodicities at its subharmonic periods (Bai and Sturrock, 1991).

Detailed analyses of the time behaviour of the different solar activity indices pointed out that the multi-peaked

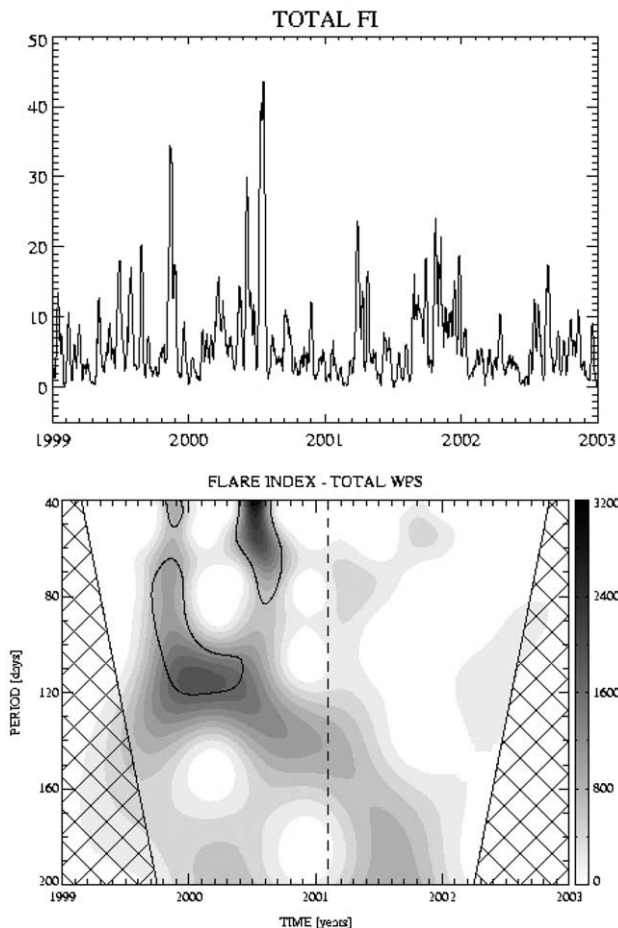


Fig. 4. The 7-day running mean of the flare index (upper panel) and the wavelet power spectrum of the daily flare index of the full disc of the Sun. Details are as Fig. 2.

structure of the solar cycle maximum is a real feature of solar activity (Bazilevskaya et al., 2000; Storini et al., 2003; Sello, 2003). The wavelet analysis demonstrated that during the maximum phase of the current solar cycle a very prominent multi-peaked structures exist in each solar hemisphere.

Flare production during this cycle was comparatively less than the previous cycle. Hence, over an 11-year solar cycle the amplification sometimes regenerates more polar field and sometimes less. At the same time, Hathaway et al. (2003) have reported strong observational evidence that a deep meridional flow towards the equator is driving the sunspot cycle. Obviously, other mechanisms, such as fluctuations in the meridional flow are believed (Hathaway, 1996) to be a product of turbulent convection and variations in the gradient of the rotation rate which was also contributing to the cycle amplitude variations. The differences on the speed of the meridional circulation during the cycles with the different amplitude and all the mechanism mentioned above can act as an intrinsic dynamics which would explain the midrange solar activity periodicities.

The solar cycle 23 with its weak magnetic activity throughout its progression merits all this detailed studies which was done with different indices. Recent research of the long-term solar variability shows that our epoch is at the onset of an upcoming minimum of the 100-year Gleissberg cycle (Bonev et al., 2004). So, it can be expected that the solar cycle 24 may be magnetically weaker than the ongoing cycle.

Acknowledgements

We thank Drs. H.E. Coffey and E.H. Erwin of WDC-A for Solar-Terrestrial Physics, NOAA E/GC2, 325 Broadway, Boulder, CO, who made the grouped flare lists available. We also thank Dr. D.H. Hathaway for the daily corrected total areas of sunspot groups, and to SIDC, RWC Belgium, World Data Center for the Sunspot Index, Royal Observatory of Belgium. The wavelet transform algorithm of C. Torrence and G.P. Compo, available at <http://paos.colorado.edu/research/wavelets/> has been used in this work. This work was supported by Boğaziçi University Research Fund by the project of 04S103 and by the Slovak grant agency VEGA (Grant 2/3015/23). This research is part of the European Solar Magnetism Network (EC/RTN contract HPRN-CT-2002-00313).

References

- Ahluwalia, H.S. The predicted size of cycle 23 based on the inferred three-cycle quasi-periodicity of the planetary index *Ap. J. Geophys. Res.* 103 (A6), 12103–12109, 1998.
- Bai, T. Periodicities in solar flare occurrence: analysis of cycles 19–23. *Astrophys. J.* 591, 406–415, 2003.
- Bai, T., Sturrock, P.A. The 154-day and related periodicities of solar activity as subharmonics of a fundamental period. *Nature* 350, 141–143, 1991.
- Bazilevskaya, G.A., Krainev, M.B., Makhmutov, V.S., Flückiger, E.O., Sladkova, A.I., Storini, M. Structure of the maximum phase of solar cycles 21 and 22. *Solar Phys.* 197, 157–174, 2000.
- Bonev, B.P., Penev, K.M., Sello, S. Long-term solar variability and the solar cycle in the 21st century. *Astrophys. J.* 605, L81–L84, 2004.
- Caballero, R., Valdes-Galicia, J.F. Galactic cosmic ray fluctuations during solar cycles 22 and 23 at high altitude neutron monitors. *Adv. Space Res.* 27, 583–588, 2001.
- Daubechies, I. *IEEE Trans. Inform. Theory* 36 (5), 961, 1990.
- Fröhlich, C., Lean, J. The sun's total irradiance: cycles, trends and related climate change uncertainties since 1976. *Geophys. Res. Lett.* 25, 4377–4380, 1998.
- Hathaway, D.H. Doppler measurements of the sun's meridional flow. *Astrophys. J.* 460, 1027–1033, 1996.
- Hathaway, D.H., Nandy, D., Wilson, R.M., Reichmann, E.J. Evidence that a deep meridional flow sets the sunspot cycle period. *Astrophys. J.* 589, 665–670, 2003.
- Kleczeck, J., *Publ. Inst. Centr. Astron.*, No. 22, Prague, 1952.
- Komitov, B.J., Bonev, B. Amplitude variations of the 11-year cycle and the current solar maximum 23. *Astrophys. J.* 554, L119–L122, 2001.

- Kumar, P., Faufoula-Georgiou, E. Wavelet analysis for geophysical applications. *Rev. Geophys.* 35, 385, 1997.
- Lou, Y.Q., Wang, Y.M., Fan, Z., Wang, S., Wang, J.X. Periodicities in solar coronal mass ejections. *Mon. Not. Roy. Astron. Soc.* 345, 809–818, 2003.
- Özgüç, A., Ataç, T., Rybák, J. Temporal variability of the flare index (1966–2001). *Sol. Phys.* 214, 375–397, 2003.
- Rybansky, M. Coronal index of solar activity I – Line 5303 Å year 1971. II – Line 5303 Å years 1972 and 1973. *Bull. Astron. Inst. Czechosl.* 26, 367–377, 1975.
- Schatten, K.H. Solar activity and the solar cycle. *Adv. Space Res.* 32, 451–460, 2003.
- Scherrer, H.P., Wilcox, M.J., Svalgaard, L., Duvall, L.T., Dittmer, H.P., Gustafson, E.K. The mean magnetic field of the sun – observations at stanford. *Sol. Phys.* 54, 353–361, 1977.
- Sello, S. Wavelet entropy and the multi-peaked structure of solar cycle maximum. *New Astron.* 8, 105–117, 2003.
- Storini, M., Bazilevskaya, G.A., Flückiger, E.O., Krainev, M.B., Makhmutov, V.S., Sladkova, A.I. The Gnevyshev gap: a review for space weather. *Adv. Space Res.* 31, 895–900, 2003.
- Torrence, C., Compo, G.P. A practical guide to wavelet analysis. *Bull. Am. Meteorol. Soc.* 79, 61, 1998.